

Analysis of A 2-Phase Stator Winding By Winding Function Methodology

*I.K.Onwuka, **U.U.Uma, *G. C. Diyoke

*Michael Okpara University of Agriculture, Umudike, Nigeria. ifeanyikayonwuka@gmail.com

**Akanulbiam Federal Polytechnic, Unwana, Nigeria.

Abstract: A two-phase stator winding is presented here and analyzed. By two-phase, it is implied that the two stator windings are identical and displaced in phase by 90 degrees, and can supply single-phase loads from either terminal. First, a stator winding was presented for a specified stator, and the winding distribution analyzed with the aim of obtaining the mmf characteristics from its functional relationship with the winding function. The particular stator winding presented in this work was found to be with low mmf harmonic level, and would perform acceptably when it forms part of an ac machine, typically, a generator of induction or reluctance type in the low power range.

Key words: Two-phase, Winding function.

I. INTRODUCTION

With the world's growing interest on reducing greenhouse effect and boosting power supply to urban and remote areas, intensive research is in the area of determining practical electromechanical conversion devices in both the low and high power ranges for easy and efficient conversion of energy from unconventional energy sources to electricity. At the low power range, such devices are required to be rugged, near maintenance free, affordable, and uncomplicated, and providing good quality of power. Along this line, extensive work has been done on single phase and three phase generators of induction and reluctance types. Self-excitation of these generators is achieved by the action of capacitors connected to the terminals of the machine. For example, [1] discussed the performance prediction and analysis of a single phase self-excited induction generator excellently. Also, [2] presented a mathematical model by which the dynamic behavior of self-excited single-phase reluctance generator can be successfully predicted under different operating conditions, while [3] was minded of the steady state analysis of the same. Plenty research results are also available in three-phase autonomous reluctance generators in both the dynamic and steady-state concerns [4, 5, 6]. Generators in the low power range are usually single-phase machines and are usually two-winding machines having a main winding and an auxiliary winding. However, less is considered of two-phase machines.

By 2-phase stator winding, it is implied here that the machine is able to supply single phase loads from the two stator terminals, with a phase difference of 90°. The analysis employed is akin to asynchronous stator winding which has a main and an auxiliary winding, of which the former has more number of turns of conductor than the latter and occupies about two thirds of the stator slots [7]. The current in both windings are displaced by an angle of 90°. The basic difference is that the windings in this work are of equal number of turns, and occupies equal number of stator slots. Such stator winding arrangement readily find application in autonomous production of electricity through renewable and non-conventional energy sources. A good design will aim to realize a sinusoidal stator mmf wave form with minimum harmonic content. Minimizing the stator mmf harmonic contents is of great importance for many reasons, including minimizing voltage and current harmonics [8]. Stator losses are also reduced. The focus of the present work is to suggest a stator winding arrangement with clear analysis, showing a sinusoidal stator mmf with reduced harmonics, of a two-phase machine. The interest is restricted to terminal rather than internal characteristics of the machine.

Specification

It is intended to obtain a stator winding design for a 1hp, 220V, 2-pole, 2-phase machine.

II. MACHINE DIMENSIONS

With the methods suggested by [7] and [9], the dimensions of the stator can be determined to meet the above specifications, with a few assumptions with respect to specific magnetic and electric loading of the machine. These are considered the main dimensions of the machine. It will be observed however, that this is a different research focus from the present endeavor.

Winding Description

A double-layer, integral-slot winding with chorded coils will be used. Taking 12 slots per pole, the stator number of slots is 24. Each slot holds 18 conductors, which could be of either or both phases. Windings were distributed as near sinusoidal as possible. References here include [7, 8, 9]. Furthermore, the windings of both phases are identical but displaced from each other by an angle of 90°. The winding clock diagram appears in figure 1. The following can easily be observed from the winding clock diagram: Number of slots = 24; Slot angular pitch = 15°; Phase belt = 10 slot pitch; Phase spread = 150°; phase shift = 90°; Number of poles = 2; Pole-pitch = 12 slots per pole.

Assumption

Each winding section is aligned axially within the air gap. This is to say that the wire is neither slanted in the circumferential direction nor tilted in the radial direction as it passes through the air gap.

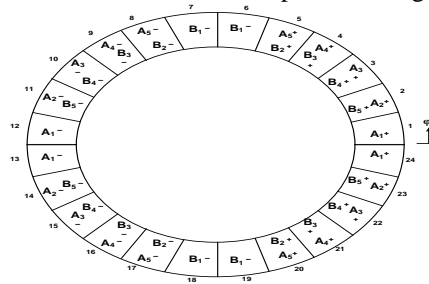


Figure 1: Winding Clock Diagram

III. WINDING FUNCTION

[10] observed that the knowledge of the winding functions for all windings together with the winding current essentially describe the spatial field distribution in the gap of the machine. Moreover, it is well known that the winding function is the basis of calculating machine inductances. Obviously, the harmonic

Table 1: The A and B-phase stator turns and winding functions

| S/No | $n_a(\phi_s)$ | Coil span | n_{ava} | $N_{as}(\phi_s)$ | $n_b(\phi_s)$ | Coil span | n_{avb} | $N_{bs}(\phi_s)$ |
|------|---------------|-------------------------------------|-----------|------------------|---------------|-------------------------------------|-----------|------------------|
| 1 | 6 | $\frac{\pi}{6} - \frac{23\pi}{12}$ | 5.250 | 0.750 | 12 | $\frac{\pi}{6} - \frac{11\pi}{12}$ | 4.500 | 7.5 |
| 2 | 9 | $\frac{\pi}{4} - \frac{11\pi}{6}$ | 7.125 | 1.875 | 9 | $\frac{\pi}{4} - \frac{10\pi}{12}$ | 2.625 | 6.375 |
| 3 | 9 | $\frac{\pi}{3} - \frac{7\pi}{4}$ | 6.375 | 2.625 | 9 | $\frac{\pi}{3} - \frac{3\pi}{4}$ | 1.875 | 7.125 |
| 4 | 12 | $\frac{5\pi}{12} - \frac{10\pi}{6}$ | 7.500 | 4.500 | 6 | $\frac{5\pi}{12} - \frac{2\pi}{3}$ | 0.750 | 5.250 |
| 5 | 18 | $\frac{\pi}{2} - \frac{19\pi}{12}$ | 9.750 | 8.250 | 0 | $\frac{\pi}{2} - \frac{7\pi}{12}$ | 0 | 0 |
| 6 | 18 | $\frac{7\pi}{12} - \frac{3\pi}{2}$ | 8.250 | 9.750 | 0 | $\frac{19\pi}{12} - \frac{7\pi}{2}$ | 0 | 0 |
| 7 | 12 | $\frac{2\pi}{3} - \frac{17\pi}{12}$ | 4.500 | 7.500 | 6 | $\frac{5\pi}{3} - \frac{41\pi}{12}$ | 5.250 | 0.750 |
| 8 | 9 | $\frac{3\pi}{4} - \frac{4\pi}{3}$ | 2.625 | 6.375 | 9 | $\frac{7\pi}{4} - \frac{10\pi}{3}$ | 7.125 | 1.875 |

| | | | | | | | | |
|----------------------|---|-------------------------------------|----------------------------|-------|--------------------------|--------------------------------------|------------------|-----------------------|
| 9 | 9 | $\frac{5\pi}{6} - \frac{5\pi}{4}$ | 1.875 | 7.125 | 9 | $\frac{11\pi}{6} - \frac{13\pi}{4}$ | 6.375 | 2.625 |
| 10 | 6 | $\frac{11\pi}{12} - \frac{7\pi}{6}$ | 0.750 | 5.250 | 12 | $\frac{23\pi}{12} - \frac{19\pi}{6}$ | 7.500 | 4.500 |
| 11 | 0 | $\pi - \frac{13\pi}{12}$ | 0 | 0 | 18 | $2\pi - \frac{37\pi}{12}$ | 9.750 | 8.250 |
| 12 | 0 | $\frac{\pi}{12} - 2\pi$ | 0 | 0 | 18 | $\frac{\pi}{12} - \pi$ | 8.250 | 9.750 |
| $\sum n_a(\phi_s) =$ | | $\sum n_{ava} = 54$ | $\sum N_{as}(\phi_s) = 54$ | | $\sum n_b(\phi_s) = 108$ | | $\sum n_{avb} =$ | $\sum N_{bs}(\phi_s)$ |

content of both stator voltage and current depend on the shape of the air gap mmf due to the stator windings. Hence, stator winding analysis based on winding function is presented here. Equation (1) represents the relationship between the air gap mmf, the winding function, and the stator current. Subscript “s” represents stator quantity, and N_s the winding function.

$$mmf_s = \frac{N_s}{2} i_s \cos \phi_s \tag{1}$$

Where ϕ_s is an angular displacement along the stator inner circumference. The winding function (WF) methodology developed in [11] was employed in this analysis. Table 1 shows the turns and winding functions for both windings, where $n(\phi_s)$ and n_{ave} are the turns function and the average turns function respectively, given by:

$$n(\phi_s) = \text{No. of turns in integration path} \tag{2}$$

$$n_{ave} = \frac{1}{2\pi} \int_0^{2\pi} n(\phi_s) d\phi_s \tag{3}$$

The winding function is then given by:

$$N_s(\phi_s) = n(\phi_s) - n_{ave} \tag{4}$$

Together with the information under the Winding Description, these equations were adjusted to develop Table 1, integrating over the span specified.

Also, figure 2 and 3 shows the actual winding function, in stair-case form. These can also be deduced from Table 1.

Harmonics Analysis

The method of Fourier series [12] was applied to obtain the various harmonics present in the winding functions expressed in Figures 2 and 3. The Fourier series of the winding function was performed and various plots obtained using the MATLAB tool [13]. The fundamental components of the winding functions for the two stator windings are:

$$N_{as} = N_s \cos(\phi_s - \delta) \tag{5}$$

$$N_{bs} = N_s \sin(\phi_s - \delta) \tag{6}$$

Where, δ is the phase shift, and subscript s refers to stator variables.

Figures 4 and 5 give a picture of the harmonic contents in the winding function, up to the 50th non-zero harmonic (odd harmonics only). This is a reflection of the distortion that will be present in the stator voltage and current waveform. It is put in better perspective by figure 6.

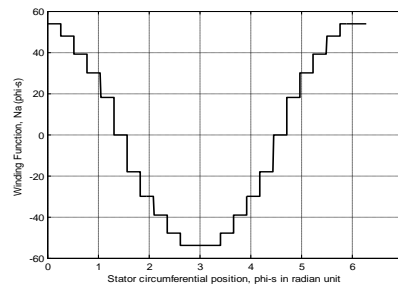


Figure 2: Actual Winding function of the a-phase winding

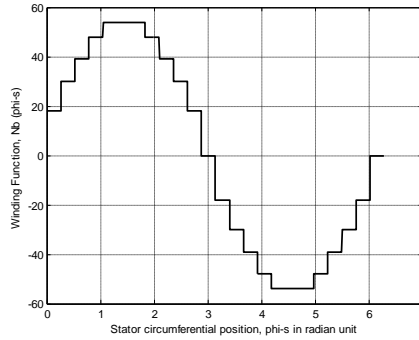


Figure 3: Actual Winding Function of the b-phase winding

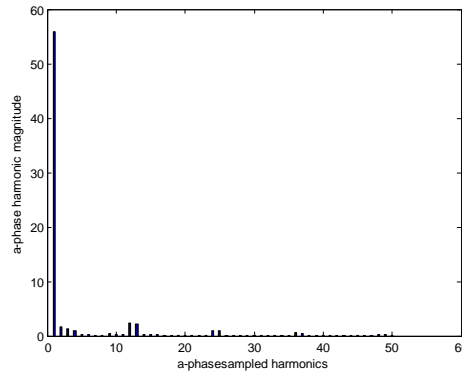


Figure 4: Harmonics of the a-phase winding function

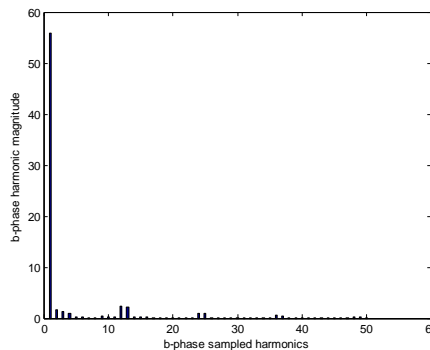


Figure 5: Harmonics of the b-phase winding function

A comparison between the resultant winding function (sum of all the harmonics including the fundamental component) and the fundamental component of the winding function, shown in figure 6, reveals that the approximation of the fundamental component to the resultant winding function is quite close. Hence, this can be used for inductance calculation of the machine. This plot is found identical for the two phases, except that they are displaced in phase by 90° . It is observed that the fundamental component is same for both windings, with the following phasor value:

$$N_{as} = 55.8254\angle - 0.1309rad \quad (7)$$

$$N_{bs} = 55.8254\angle 1.4399rad \quad (8)$$

If the close approximation of the fundamental harmonic to the resultant winding function is accepted as the eventual winding function, then the effective number of stator turns will be taken as $N_s = 55.8254$. It is clear that the influence of winding design features which have not been considered in the analysis are accounted for in N_s .

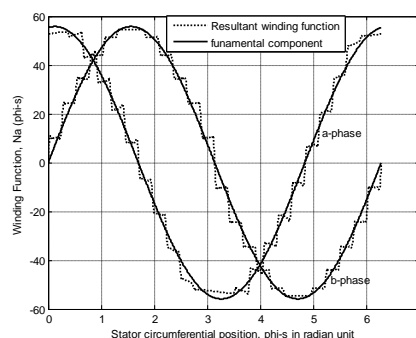


Figure 6: Comparison between the resultant winding function and the fundamental component of the function.

IV. CONCLUSION

It must be observed here that saliency has no influence on the form of the winding function [10], so that the stator winding here realized can be adapted to a round-rotor or a salient-pole machine. The particular design of the stator winding presented in this work suggests minimal current and voltage harmonics. Also, the analysis here presented shows that with little loss of accuracy, the fundamental component of the winding function can be adopted for inductance calculation of the machine. Again, it is clear that the two-phase stator presented in this work will perform acceptably when it forms part of an electric machine, typically, a small generator. As earlier mentioned, this generator could be of induction or reluctance type. It is therefore presented here that a two-phase ac generator of various power ratings can be designed and used for domestic and certain farm processing activities in the low power range. The authors think this will lead to a better utilization of the stator slots.

REFERENCES

- [1]. Bhim Singh et al, "Improved Steady State and Transient performance with optimum excitation of Single-phase self-excited Induction Generator", *Electric Machines and Power Systems*, 28:591-604, 2000.
- [2]. S.M. Allam, M. A. El-Khazendar, and A.M. Osheiba. Dynamic analysis of a self-excited single-phase reluctance generator, *Electric Power Components and Systems*, 34:725-738, 2006.
- [3]. J. Chen and P. Famouri. Single-phase self-excited reluctance generator, part I: Steady-state analysis, *Electr. Power Component Systems*, vol. 31, pp. 129-147, 2003.
- [4]. Ben-Hail, N., and Rabinovici, R., "Three-phase autonomous reluctance generator", *IEEE Proc. Elect. Power Appl.*, Vol. 148, No. 5, pp. 438-442, September 2001.
- A. K. Tandon, S. S. Murthy, and G. J. Berg. Steady-state analysis of capacitor self-excited induction generators, *IEEE Transactions on Power Apparatus and Systems*, vol. PAS-103, no. 3, pp. 612-618, March 1984.
- [5]. T. F. Chan. Steady-state analysis of a three-phase self-excited reluctance generators, *IEEE Transactions on Energy Conversion*, vol. 7, no. 1, pp. 223-230, March 1992.
- [6]. Mittle, V. N., and Mittal A., "Design of Electrical Machines", Standard Publishers Distributors, Delhi, 2006.
- [7]. Paul C. Krause, Oleg Wasynczuk, Scott D. Sudho. Analysis of Electric Machinery, IEEE Press, New York, 1995.
- [8]. JuhaPyrhonen, TapaniJokinen, Valeria Hrabovcova, "Design of Rotating Electric Machines", John Wiley and Sons Ltd, 2008.
- [9]. P. S. Bimbhra, "Electrical Machinery", Khana Publishers, Delhi, Seventh Edition, 2008.
- [10]. Obe, E. S. Nnadi, D. B and Eke, J. Inductances and Airgap Flux density of a Synchronous Reluctance Machine using the Actual Machine Geometry, *NSE Technical Trans.* Vol. 44. No. 4, pp.49-63, 2009.
- [11]. Erwin Kreyszig. Advanced Engineering Mathematics, John Wiley and Sons, Inc, New York, 1979.
- [12]. MATLAB. Mathworks 2007 :Natic, Pennsylvania, USA.